Inorganic Chemistry

ARTICLE

pubs.acs.org/IC

# Formation of Zn(II) and Cd(II) Coordination Polymers Assembled by Triazine-Based Polycarboxylate and *in-Situ*-Generated Pyridine-4-thiolate or Dipyridylsulfide Ligands: Observation of an Unusual Luminescence Thermochromism

Qilong Zhu,[†,‡] Tianlu Sheng,[†] Chunhong Tan,[†,‡] Shengmin Hu,[†] Ruibiao Fu,[†] and Xintao Wu*[,†]

[†]State Key Laboratory of Structural Chemistry, Fujian Institute of Research on the Structure of Matter, The Chinese Academy of Sciences, Fuzhou, Fujian 350002, China

[‡]Graduate University of the Chinese Academy of Sciences, Beijing 100039, China

Supporting Information

**ABSTRACT:** Three novel coordination polymers, $[Cd_5(HTTHA)_2(Hpt)_4(H_2O)]\cdot 4H_2O$ (**1**; $H_6TTHA$ = 1,3,5-triazine-2,4,6-triamine hexaacetic acid, Hpt = pyridinium-4-thiolate), $\{[Cd_3(TTHA)(dps)(H_2O)_3]_2\}\cdot H_2O$ (**2**), and $[Zn_3(TTHA)(dps)(H_2O)]\cdot 5H_2O$ (**3**; dps =4,4′-dipyridylsulfide), have been synthesized by the flexible hexapodal acid $H_6TTHA$ and *in-situ*-generated Hpt and dps ligands from a 4,4′-dipyridyldisulfide (dpds) precursor through cleavage of both S−S and S−C($sp^2$) bonds and temperature-dependent chemical rearrangement under hydrothermal conditions. Polymers **2** and **3** exhibit 3D frameworks, while in **1**, the extended 3D network can be described as 2D layers further bridged via H-bond interaction. Intriguingly, the three compounds have shown an unusual luminescence thermochromism. Upon decreasing the temperature from 298 to 10 K, the emission bands grow in intensity and change in color dramatically.

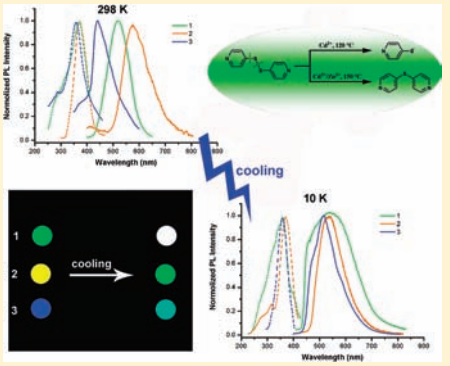


## INTRODUCTION

Since the first example of solvothermal *in situ* ligand reaction on the rearrangement of 2,2′-dipyridylamine into dipyrido-[1,2-*a*:2′,3′-*d*]imidazole was reported by Li et al. in 1998,[1] *in situ* ligand reactions, as a very important research field, have recently been extensively investigated for discovery of new organic reactions and metal−organic polymers that exhibit intriguing structures and promising properties for potential applications.[2] The combination of hydro(solvo)thermal methods with *in situ* synthesis has been proven to be an effective alternative synthetic route to achieve coordination compounds that otherwise are inaccessible in normal direct preparation from the ligands.[3] Until now, quite a few *in situ* ligand reactions, including C−C bond formation, hydroxylation, tetrazole and triazole formation, substitution of aromatic groups, as well as cleavage and formation of S−S bonds, have been reported.[1b,2a−2c] However, to exert synthetic control of our target products from hydrothermal reactions is not a trivial task. The elucidation of reaction mechanisms also faces serious challenges.[4]

The reversible cleavage of the disulfide bond is universally reflected in various biological processes such as protein folding and unfolding. Although the hydro(solvo)thermal system tends to favor the oxidative formation of the disulfide bond, the reductive cleavage of the disulfide bond also has been explored recently as an attractive route to functional materials.[5] 4,4′-Dipyridyldisulfide (dpds), which tends to adopt the pyridyl form coordinating with metal atoms through the nitrogen donor without S−S bond cleavage in most coordination polymers, has attracted intense attention.[6] This is because some novel coordination polymers featuring various *in situ* spacers, including pyridine-4-thiolate (pt), 4,4′-dipyridylsulfide (dps), 4,4′-dipyridyltrisulfide (dpts), and 1-(4-pyridyl)-4-thiopyridine (ptp), ensuing from the chemical rearrangement of the starting dpds reagent have been developed.[7] Meanwhile, these compounds containing $d^{10}$ metals usually possess attractive luminescent properties, particularly the important temperature-dependent emission feature (luminescence thermochromism).[7a,b,8] Their luminescent wavelengths and intensities involved in different charge-transfer mechanisms can be modulated at various temperatures. Although a lot of investigations about Cu(I) and Ag(I) coordination polymers exhibiting luminescence thermochromism have been carried out, few examples involving Cd(II) and Zn(II) have been reported.[9] In our previous work, the flexible hexapodal ligand 1,3,5-triazine-2,4,6-triamine hexaacetic acid ($H_6TTHA$) has been proven to be a good fluorophore ligand.[10] Herein, two other unusual *in situ* transformations of dpds were observed in the hydrothermal reactions of two $d^{10}$ metal salts and dpds with $H_6TTHA$ at different temperature, giving a 2D coordination network of $[Cd_5(HTTHA)_2(Hpt)_4(H_2O)]\cdot 4H_2O$ (**1**) at

**Received:** March 29, 2011
**Published:** July 11, 2011

 © 2011 American Chemical Society 

120 °C and two 3D coordination networks of $\{[Cd_3(TTHA)(dps)(H_2O)_3]_2\}\cdot H_2O$ (**2**) and $[Zn_3(TTHA)(dps)(H_2O)]\cdot 5H_2O$ (**3**) at 150 °C, respectively. All three compounds show bright luminescence both at ambient temperature and freezing conditions, and drastic color changes and luminescence enhancement when the temperature is lowered. This can open up to promising applications in the area of luminescent materials.

## EXPERIMENTAL SECTION

**Materials and Measurements.** All reagents and solvents used were received from commercial suppliers without further purification. Elemental analyses (C, H, and N) were performed with a Vario MICRO CHNOS elemental analyzer. The infrared spectra with KBr pellet were recorded in the range 4000−400 $cm^{-1}$ on a Perkin-Elmer Spectrum One FT-IR spectrometer. Thermal analyses were performed on a NETZSCH STA 449C instrument from room temperature to 1000 °C with a heating rate of 10 °C $min^{-1}$ under nitrogen flow. The solid-state luminescence emission/excitation spectra were recorded on a FLS920 fluorescence spectrophotometer equipped with a continuous Xe-900 xenon lamp and a $\mu$F900 microsecond flash lamp. For low-temperature measurements, microcrystalline samples were mounted on a closed cycle helium cryostat. Powder XRD patterns were acquired on a DMAX-2500 diffractometer using Cu K$\alpha$ radiation at ambient environment. The calculated patterns were generated with PowderCell.

**Synthesis.** The ligand 1,3,5-triazine-2,4,6-triamine hexaacetic acid ($H_6$TTHA) was synthesized according to the method described in the literature.[11]

**$[Cd_5(HTTHA)_2(Hpt)_4(H_2O)]\cdot 4H_2O$ (1).** $Cd(NO_3)_2\cdot 4H_2O$ (278 mg, 0.9 mmol) and dpds (66 mg, 0.3 mmol) were added to the solution of $H_6$TTHA (142 mg, 0.3 mmol in 10 mL of water) which was first adjusted to an acidity of pH ∼ 6 by adding the solution of sodium hydroxide. Then, the suspension was transferred into a Teflon-lined autoclave (20 mL). The autoclave was heated and kept at 120 °C for 3 days, then slowly cooled to 30 °C at about 5 °C $h^{-1}$. Yellowish, rhombic, platelike single crystals were obtained which were filtered, washed with distilled water, and used for the X-ray diffraction determination. Yield: 56% on the basis of $H_6$TTHA. Anal. Calcd for $Cd_5C_{50}H_{56}N_{16}S_4O_{29}$: C, 29.51; H, 2.77; N, 11.01%. Found: C, 29.30; H, 2.74; N, 10.05%. IR (KBr, $cm^{-1}$): $\upsilon_{O-H,C-H}$ = 3430 (vs, br), 3428 (s), 3225 (s), 3124 (s), 2933 (s), and 2851 (s); $\upsilon_{C=C,C=N}$ = 1727 (m); $\upsilon_{C=O}$ = 1593 (vs) and 1557 (vs); $\delta_{C-H}$ = 1477 (s), 1428 (m), 1385 (s), and 1300 (m); $\upsilon_{C-C,C-N}$ = 1264 (m), 1195 (m), and 1116 (m); $\delta_{Ar-H}$ = 987 (w), 812 (w), 716 (w), and 628 (m); $\upsilon_{C-S}$ = 484 (w).

**$\{[Cd_3(TTHA)(dps)(H_2O)_3]_2\}\cdot H_2O$ (2).** $Cd(NO_3)_2\cdot 4H_2O$ (278 mg, 0.9 mmol) and dpds (66 mg, 0.3 mmol) were added to the solution of $H_6$TTHA (142 mg, 0.3 mmol in 10 mL of water) which was first adjusted to an acidity of pH ∼ 5.5 by adding the solution of sodium hydroxide. Then, the suspension was transferred into a Teflon-lined autoclave (20 mL). The autoclave was heated and kept at 150 °C for 3 days, and then slowly cooled to 30 °C at about 5 °C $h^{-1}$. Yellowish, needlelike single crystals were obtained which were filtered, washed with distilled water, and used for the X-ray diffraction determination. Yield: 79% on the basis of $H_6$TTHA. Anal. Calcd for $Cd_6C_{50}H_{54}N_{16}S_2O_{31}$: C, 28.41; H, 2.58; N, 10.60%. Found: C, 28.22; H, 2.55; N, 10.52%. IR (KBr, $cm^{-1}$): $\upsilon_{O-H,C-H}$ = 3234 (vs, br); $\upsilon_{C=O}$ = 1577 (vs) and 1536 (s); $\delta_{C-H}$ = 1492 (s), 1411 (s), 1390 (s), and 1298 (s); $\upsilon_{C-C,C-N}$ = 1282 (m), 1264 (m), 1184 (m), and 1065 (w); $\delta_{Ar-H}$ = 812 (m), 739 (m), 672 (w), 640 (m), and 615 (m); $\upsilon_{C-S}$ = 534 (w) and 493 (w).

**$[Zn_3(TTHA)(dps)(H_2O)]\cdot 5H_2O$ (3).** $Zn(NO_3)_2\cdot 6H_2O$ (268 mg, 0.9 mmol) and dpds (66 mg, 0.3 mmol) were added to the solution of $H_6$TTHA (142 mg, 0.3 mmol in 10 mL of water) which was first adjusted to an acidity of pH ∼ 6 by adding the solution of sodium hydroxide. Then, the suspension was transferred into a Teflon-lined autoclave (20 mL). The autoclave was heated and kept at 150 °C for 3 days, and then slowly cooled to 30 °C at about 5 °C $h^{-1}$. Yellowish, block single crystals were obtained which were filtered, washed with distilled water, and used for the X-ray diffraction determination. Yield: 76% on the basis of $H_6$TTHA. Anal. Calcd for $Zn_3C_{25}H_{32}N_8SO_{18}$: C, 31.25; H, 3.36; N, 11.66%. Found: C, 30.96; H, 3.31; N, 11.54%. IR (KBr, $cm^{-1}$): $\upsilon_{O-H,C-H}$ = 3854 (w), 3747 (w), 3444 (vs, br), 3094 (m), 2994 (m), and 2934 (m); $\upsilon_{C=O}$ = 1591 (vs), 1566 (vs), and 1540 (s); $\delta_{C-H}$ = 1489 (s), 1421 (m), 1385 (s), and 1315 (m); $\upsilon_{C-C,C-N}$ = 1285 (m), 1255 (s), 1213 (m), 1063 (w), 1025 (w), and 990 (m); $\delta_{Ar-H}$ = 813 (m), 731 (m), and 656 (m); $\upsilon_{C-S}$ = 546 (w) and 493 (w).

**Scheme 1. Schematic Representation of the *in Situ* Ligand Reactions**

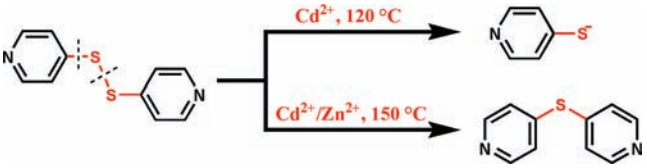


**X-ray Crystallographic Study.** Data collection was performed at 293(2) K on Rigaku Mercury CCD diffractometer with graphite-monochromated Mo K$\alpha$ ($\lambda$ = 0.710 73 Å) radiation at room temperature. The structures were solved by direct methods and refined by the full-matrix least-squares on $F^2$ using the SHELXTL-97 program.[12] All non-hydrogen atoms were refined with anisotropic displacement parameters. Hydrogen atoms attached to carbon atoms were placed in geometrically idealized positions and included as riding atoms (C−H bond fixed at 0.97 Å), and the hydrogen atoms of the water molecules could not be reliably located but are included in the formula. Notably, O4W in compound **2** was refined by using the "ISOR" restraint to make the ADP values of the disordered atoms more reasonable. Crystallographic data and structure determination summaries are summarized in Tables S1−3. And the selected bond lengths and angles of the complexes are listed in Tables S4−6.

## RESULTS AND DISCUSSION

**Synthesis.** The construction of coordination networks based on dpds usually occurs without any changing of the dpds precursor, although several examples in which disulfides can undergo cleavage and formation of S−S and S−C($sp^2$) bonds under various thermal, chemical, photochemical, and electrochemical conditions have been found recently.[7a,13] In our case, the starting dpds reagent was unprecedentedly converted into pyridine-4-thiolate (pt) and 4,4′-dipyridylsulfide (dps) ligands (Scheme 1). Compound **1** was successfully obtained from the hydrothermal reaction of $H_6$TTHA, dpds, and cadmium ion at 120 °C where the starting dpds can be converted into a zwitterionic functional pt ligand characteristic of mixed nitrogen and sulfur donors. When the same reaction as that of **1** was carried out at 150 °C except for little higher acidity, compound **2** was isolated, and concomitantly the dpds was converted into another new dps ligand. However, once cadmium ion was displaced by zinc ion, only *in situ* compound **3** was obtained at 120−150 °C with a field maximum at 150 °C. Similar to the photochemical reaction of dpds,[14] we believe that the initial stage of the mechanism of the *in situ* reaction involved formation of radicals of 4-pyridyl, 4-thiopyridyl, 4-dithiopyridyl, and sulfur (Scheme S1). Recombination of these radicals led to the formation of pyridine-4-thiolate and 4, 4′-dipyridylsulfide. On account

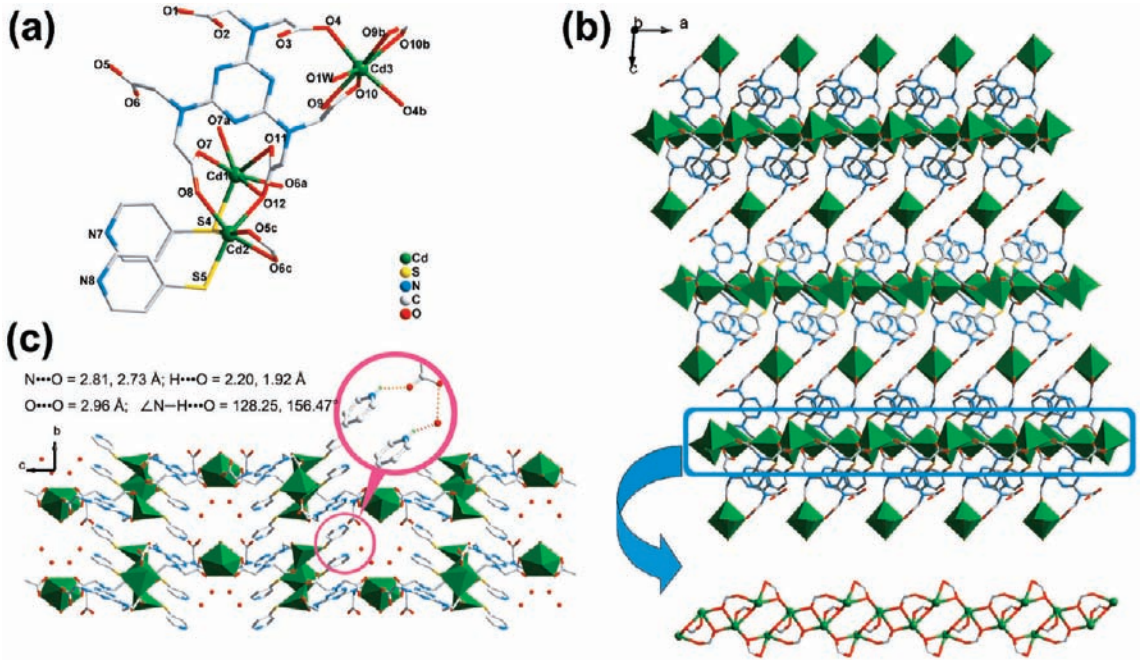


**Figure 1.** (a) Coordination environment of the Cd(II) ions in compound **1**. Hydrogen atoms have been omitted for clarity. Symmetry codes for the generated atoms: a, 2.5 − *x*, 0.5 − *y*, −*z*; b, 3 − *x*, *y*, −0.5 − *z*; c, 1 + *x*, *y*, *z*. (b) View of the 2D network in compound **1** constructed from 1D inorganic chains cross-linked via the $TTHA^{6-}$ ligands and the mononuclear Cd ions. (c) Top view of the 3D extended framework along *a*-axis in compound **1** *via* H-bond linkages among layers.

of these phenomena and an earlier report by Tong and coworkers,[1b] the energy barrier in the formation of dps should be larger than that of pt, and the temperature plays a critical role; in addition, the different metal ions may be correlated to the formation of final products.

**Structure of 1.** A single-crystal X-ray diffraction reveals that compound **1** is a 2D network, and the fundamental building unit consists of three independent Cd(II) centers, and two protonated pyridinium-4-thiolate (Hpt) ligands and a $TTHA^{6-}$ ligand (Figure 1a). The Cd1 and Cd2 are both located in distorted $[CdO_5S]$ octahedral coordination environments. Three carboxylate oxygen atoms (O7a/O11/O12 and O5c/O6c/O8) and a terminal sulfur atom (S4) of Hpt constitute the basal plane of the octahedrons, while the two polar sites are completed by O6a/O7 and O12/S5, respectively. The bond lengths of Cd−O and Cd−S are in the ranges 2.241(4)−2.458(4) and 2.514(2)−2.895(1) Å, respectively. Different from Cd1 and Cd2, Cd3 adopts a distorted pentagonal bipyramidal $[CdO_7]$ coordination geometry with two carboxylate oxygen atoms O4 and O4b at the apical positions and other five oxygen atoms composing the equatorial planes. The Cd−O distances fall within the range from 2.346(6) to 2.463(5) Å. It is interesting that the Cd1 and Cd2 are connected to 1D metal chains, in which two different rings are arranged alternately (Figure 1b). The inorganic chains furnished with $TTHA^{6-}$ ligands were interconnected by the mononuclear Cd3 into 2D layers which are further bridged *via* H-bond interaction extending to a 3D network (Figure 1c). Due to the flexibility, the six arms of $TTHA^{6-}$ ligands show significant deviation from the central triazine rings to form the enantiomeric pairs of ligand (Figure S1), which also can be found in previous compounds.[10a,15] The terminal coordination pyridine-4-thiolate species are protonated, restraining from extending in the other direction, which may be the cause of the 2D network.

**Structure of 2.** X-ray diffraction analysis discloses that compound **2** crystallizes into the noncentrosymmetric orthorhombic space group *Fdd*2 with Flack parameter of 0.02(3), showing a 3D network. As illustrated in Figure 2a, the asymmetric unit contains three Cd(II) centers, a 4,4′-dipyridylsulfide (dps) ligand and a $TTHA^{6-}$ ligand. The Cd1 and Cd3 are surrounded by five oxygen and one pyridine nitrogen atoms into distorted $[CdO_5N]$ octahedral coordination geometries with O7c/N8d and O2W/O3 at the apical positions, respectively. The Cd2 is seven-coordinated by carboxylate oxygen atoms with a distorted capped octahedral coordination environment. The distances between Cd and coordination atoms are in the range 2.258(5)−2.619(5) Å. Intriguingly, these metal ions are connected into infinite metal chains by the bridging carboxylate oxygen atoms. The chains are bridged by the *syn*−*anti* carboxylate groups of $TTHA^{6-}$ to form a 3D hybrid framework which is further furnished with the dps and $TTHA^{6-}$ ligands (Figures 2b and S2). Unlike the above-mentioned chiral configurations of $TTHA^{6-}$ ligands, the ligands in compound **2** are mirror symmetric. Nevertheless, the *in-situ*-generated dps ligand, acting as the bridging "spacers", is bent around the sulfur atom with some flexibility. The torsion angle of the dps (∠C−S−C) is 103.354(2)°, and the dihedral angle of two aromatic rings is 69.700(0)°.

**Structure of 3.** As shown in Figure 2c, the asymmetric unit of compound **3** includes three crystallographically independent Zn(II) ions which are all located in a tetrahedral coordination environment. The Zn−O and Zn−N bond lengths in the three tetrahedrons are in the ranges 1.928(4)−2.007(4) and 2.015(4)−2.055(5) Å, respectively. The 3D network can be described as a special framework constructed from the flexible hexapodal $TTHA^{6-}$ ligands and the Zn(II) ions with microchannels which are obstructed by dps acting as obstacles (Figure 2d). The six


dx.doi.org/10.1021/ic200640g |*Inorg. Chem.* 2011, 50, 7618–7624

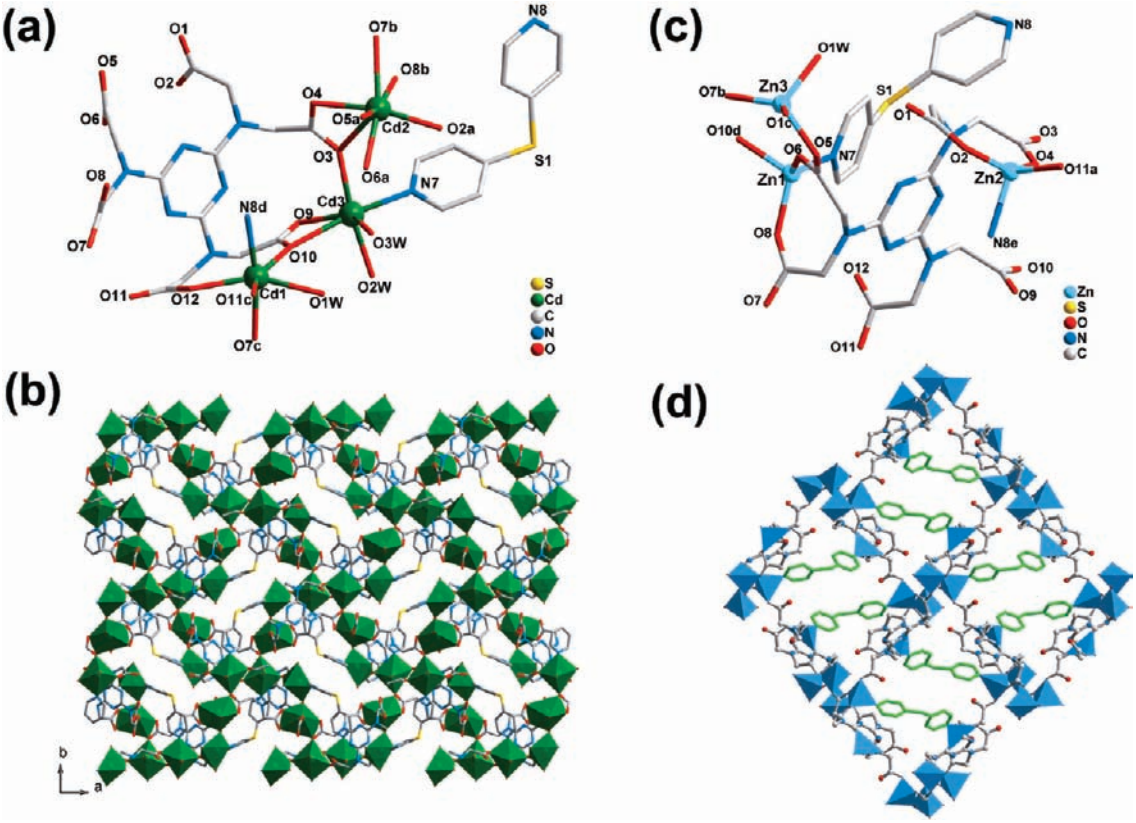


**Figure 2.** (a) Coordination environment of the Cd(II) ions in compound **2**. Hydrogen atoms have been omitted for clarity. Symmetry codes for the generated atoms: a, *x*, *y*, 1 + *z*; b, 0.25 + *x*, 0.75 − *y*, 0.75 + *z*; c, −*x*, 0.5 − *y*, 0.5 + *z*; d, −0.25 + *x*, 0.75 − *y*, −0.75 + *z*. (b) View of the 3D network packing along *c*-axis in compound **2**. (c) Coordination environment of the Zn(II) ions in compound **3**. Hydrogen atoms have been omitted for clarity. Symmetry codes for the generated atoms: a, −1 + *x*, *y*, *z*; b, 1 − *x*, −*y*, 2 − *z*; c, −*x*, −*y*, 2 − *z*; d, 1 − *x*, −0.5 + *y*, 1.5 - *z*; e, *x*, 0.5 − *y*, 0.5 + *z*. (d) View of the 3D framework along *c*-axis with the highlighted dps ligands as green in compound **3**.

arms of each chiral configuration of the $TTHA^{6-}$ ligands are arranged in the same way as the ones in compound **1** based on the planes of the triazine rings. Meanwhile, the certain flexibility of dps also can be found in this structure whose torsion angles (∠C−S−C) and dihedral angles of two aromatic rings are 106.235(2)° and 74.221(0)°, respectively.

**Thermal Stabilities.** The thermal stability of these compounds was investigated through TGA experiments in the temperature range 30−1100 °C under a flow of nitrogen. A slow weight loss for compound **1** in the temperature range 60−150 °C was attributed to the loss of the four free and a coordination water molecules (calcd 4.42%, found 4.48%). From then on, almost no loss was observed until 285 °C, at which temperature the compound began to decompose. For compound **2**, this loss of the one free and six coordination water molecules from 156 to 270 °C was significant (calcd 5.96%, found 6.13%), and the rapid weight loss occurred at *ca.* 375 °C, suggesting further the decomposition of compound **2**. TGA curve of compound **3** illustrates that there was a sharp weight loss stage between 45 and 110 °C due to the loss of all the five free water molecules (calcd 9.37%, found 9.11%). The removal of organic components started from 410 °C.

**Luminescent Properties.** Photoluminescence properties of compounds **1**−**3** were investigated, showing their intense emission in the solid state under near-UV excitation. It is known that some fluorescent coordination polymers are sensitive to the local coordination geometry of metal centers and measurement temperature,[16] which is also reflected on the three compounds. The solid-state emission spectrum of compound **1** at room temperature displays an intense emission band centered on 520 nm with excitation maximum at 368 nm (Figure 3a). Quantum yield, $\Phi_f$, is a measure of the emission efficiency of a fluorochrome. The quantum yield of **1** was determined by means of an integrating sphere and was found to be 1.17%. The solid-state lifetime at room temperature is in the range of nanoseconds (Table 1), suggestive of its fluorescent character. According to decay lifetimes and related thiolate−metal complexes, the green emission should be assigned to originate from LMCT (S→Cd).[17] To investigate the effects of measurement temperature, the emission spectra of **1**−**3** were also recorded at low temperature, showing interesting luminescence thermochromism, and the data are listed in Table 1. As the temperature is decreased to 10 K, compound **1** gives rise to a broad emission band nearly covering the entire visible spectrum from 415 to 750 nm (Figure 3b). Its quantum yield significantly increases to 16.02% when excited by 360-nm light. The CIE (Commission International de L'Eclairage) 1931 chromaticity coordinates of the white-light emission are approximately (0.34, 0.36), close to that of pure white light (Figure 3c). Among the reported thiolate−metal coordination polymers, they almost show similar emission maxima at room temperature and a certain degree of blue shifts without significant changes of the emission-band shapes at low temperature.[17,18] This should be the first example of a thiolate−metal compound showing broad emission throughout the full visible spectrum when frozen. Hence, the fluorescence of **1** is


dx.doi.org/10.1021/ic200640g |*Inorg. Chem.* 2011, 50, 7618–7624

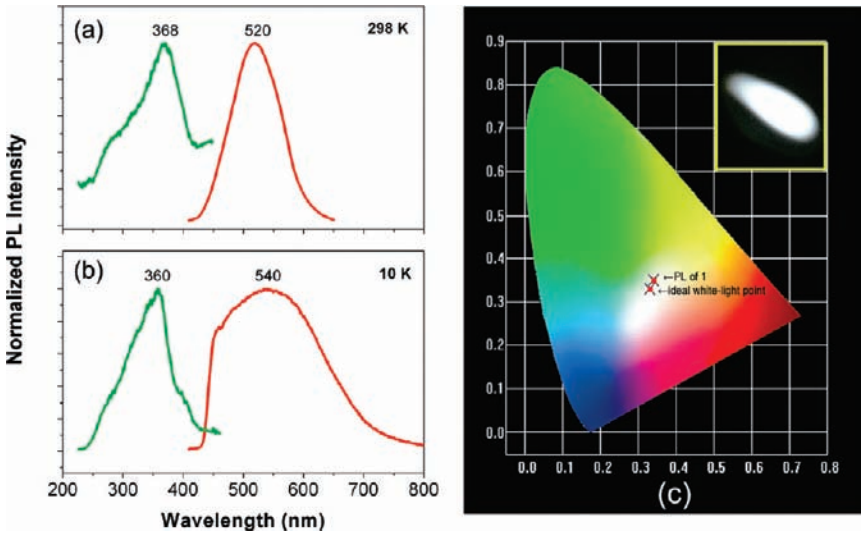


**Figure 3.** Normalized emission (red) and excitation (green) spectra of compound **1** collected in the solid state (a) at room temperature and (b) 10 K, respectively. (c) CIE-1931 chromaticity diagram showing the white fluorescence of **1** at 10 K. The CIE coordinates for the emission are (0.34, 0.36). CIE coordinates are calculated using the software GoCIE obtained from http://www.geocities.com/krjustin/gocie.html. The ideal white-light point is at (0.33, 0.33). Inset: fluorescent image of the "white" luminescing compound **1** at 10 K.

**Table 1. PL Data of Compounds 1−3 at Room Temperature (rt) and 10 K**

| | $\lambda_{ex}$/nm | | $\lambda_{em}$/nm | | $\Phi_f$ (%) | | |
|---|---|---|---|---|---|---|---|
| compd | rt | 10 K | rt | 10 K | rt | 10 K | $\tau$/ns (rt) |
| **1** | 368 | 360 | 520 | 540 | 1.17 | 16.02 | 0.44 |
| **2** | 370 | 370 | 580 | 538 | 3.75 | 31.23 | 1.32 |
| **3** | 357 | 354 | 440 | 455, 512 | 10.88 | 28.42 | 1.47 |

tunable from green to white on the basis of the variation of measurement temperature.

The spectrum of compound **2** at room temperature shows an intense emission band at 580 nm under excitation at 370 nm (Figure 4). The quantum yield for the yellow emission reaches 3.75%; and the lifetime of the emission is also consistent with the nanosecond scale of fluorescence. The emission property of luminophore dps has been investigated previously showing a weak, broad emission band centered at 536 nm.[19] Due to the similar shape and energy of emission bands for both free dps and metal complex, the emission band in **2** is tentatively assigned to intraligand charge transfer (ILCT). We found quite similar luminescent properties for reported Ag(I) and Cu(I) complexes containing the luminophore dps where the transition originates from ILCT excited states.[19,20] However, in the case of two related Zn(II) polymers $[Zn(dps)(CH_3COO)_2]$ and $[Zn(dps)_2(H_2O)_2](ClO_4)_2 \cdot H_2O$, the intraligand bands are blue-shifted to 356 and 397 nm.[19a] The variations of these emissions may result from the changes of the conformation and the central metal ions. At 10 K, a blue shift of 42 nm is observed with respect to the emission band of compound **2** at room temperature, while its full width at half-maximum (fwhm) value undergoes no change. The intensity of the emission response sharply rises to $\Phi_f$ = 31.23%. Figure 4 shows the emission spectra of **2** recorded at different temperature. The 370-nm excitation maximum remains unchanged with decreasing temperature (Figure S3), while the intensity and blue shift of the emission signal vary linearly, which

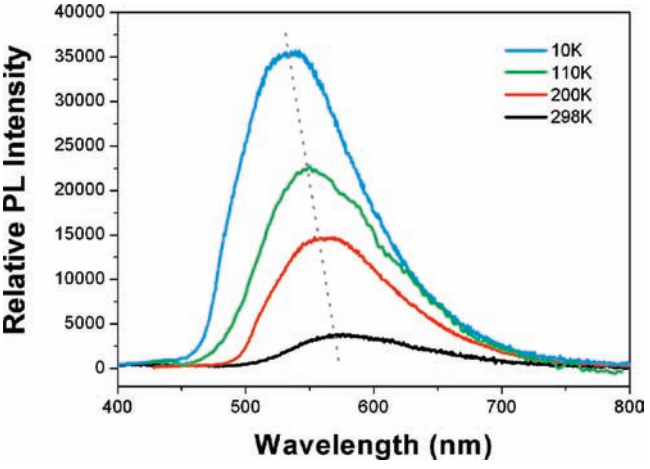


**Figure 4.** Relative emission spectra of compound **2** collected with excitation at 370 nm in the solid state at different temperature.

reveals that compound **2** will be a potential candidate for applications in temperature-sensing devices.[21]

On the other hand, the photoluminescent properties of **3** are quite different from those of **1** and **2**. The free $H_6$TTHA ligand luminesces in the solid state with an emission maximum at 425 nm (Figure S4), and the blue emission band is not strongly perturbed upon its coordination to Zn(II) in compound **3** with a red shift of 15 nm (Figure 5). Thus, the band at 440 nm with a nanosecond lifetime should be interpreted as the metal-perturbed intraligand transition. The quantum yield of **3** is 10.88% under excitation at 357 nm which appears to exhibit much better performance than most of the reported triazine-based coordination polymers.[22] In compound **3**, the second ligand dps is not likely to interfere with the charge-transfer process compared with it in compound **2** at room temperature, which may be related to the fact that it has a larger dihedral angle between the pyridine rings of the dps ligand (**2**, 69.7°; **3**, 74.2°). For compound **3** at 10 K, excitation at 357 nm gives an intense green emission with


dx.doi.org/10.1021/ic200640g |*Inorg. Chem.* 2011, 50, 7618–7624

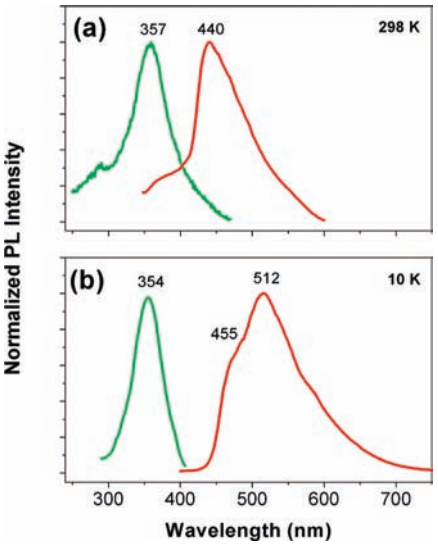


**Figure 5.** Normalized emission (red) and excitation (green) spectra of compounds **3** collected in the solid state (a) at room temperature and (b) at 10 K, respectively.

maximum and shoulder bands at 512 and 462 nm, which possibly originates from two intraligand transitions of $TTHA^{6-}$ and dps ligands, respectively. The appearance of the new 512-nm band is partly attributable to a significant reduction in the rate of nonradiative decay in the process of a $\pi \rightarrow \pi^*$ transition of dps at low temperature. Compared with compound **2** at 10 K, the blue shift of 24 nm can be attributed to its larger dihedral angle between the pyridine rings of the dps ligand which could reduce the delocalization of $\pi$ electrons and increase the energy gap between the $\pi^* - \pi$ molecular orbital of dps. The quantum yield of **3** was found to mount up to 28.42% at 10 K.

Temperature-dependent behaviors have been observed for the luminescent spectra of each complex studied herein. In some cases, the structures of coordination polymers are temperature-dependent. The different structures at different temperatures might cause the emission changes.[23] Under a cold nitrogen gas stream from a cryostat (close to 100 K), the crystallographic data of the three samples have been collected, but found to show no essential change compared with those at room temperature (Tables S1−3). However, the slight shrinkage of the unit cell sizes at low temperature was observed which may partly cause the tremendous changes of the emission bands. At the same time, cold should be favorable for the rigidity of ligands, thereby reducing the radiationless decay of the intraligand ($\pi \cdots \pi^*$) excited state to some extent, thus helping to increase the quantum yields. So far, luminescence thermochromism of coordination polymers has been encountered in polynuclear Cu(I) and Ag(I) complexes and was associated with variations of the intermetallic distances between two metal centers within the clusters in the excited state,[9] while investigations of the Cd(II) and Zn(II) coordination polymers exhibiting luminescence thermochromism have been rare, and some mechanisms remain unclear.

## CONCLUSIONS

In summary, three novel coordination polymers have been hydrothermal synthesized by *in-situ*-generated pyridinium-4-thiolate (Hpt) and 4,4′-dipyridylsulfide (dps) ligands from the 4,4′-dipyridyldisulfide (dpds) precursor through the cleavage and formation of S−S and S−C($sp^2$) bonds. Interestingly, the three polymers all show favorable luminescence thermochromism. In particular, compound **1** during freezing even produces a modification in the emission color from green to white, while compound **2** undergoes linear variation in intensity and in color with temperature. However, compound **3** exhibits different charge-transfer mechanisms at various temperatures and, consequently, the luminescent properties. Facile synthesis, moderate thermal stability, high fluorescent intensity, easy separation, and temperature-dependent emission make the three compounds good candidates for display and lighting applications.

## ASSOCIATED CONTENT

**Supporting Information.** X-ray crystallographic files in CIF format, additional figures, excitation and emission spectra, simulated and experimental XRD powder patterns, TGA curves, and selected bond lengths and angles. This material is available free of charge via the Internet at http://pubs.acs.org.

## AUTHOR INFORMATION

### Corresponding Author

*E-mail: wxt@fjirsm.ac.cn. Fax: (+86)591-83714947. Phone: (+86)591-83719238.

## ACKNOWLEDGMENT

This research was supported by grants from the 973 Program (2007CB815301), the National Science Foundation of China (21073192, 20733003, 20871114, and 20801055), the Science Foundation of CAS (KJCX2-YW-H20), and the Science Foundation of Fujian Province (2009HZ0006-1 and 2006L2005).

## REFERENCES

(1) (a) Lu, J. Y.; Cabrera, B. R.; Wang, R. J.; Li, J. *Inorg. Chem.* **1998**, *37*, 4480–4481. (b) Chen, X. M.; Tong, M. L. *Acc. Chem. Res.* **2007**, *40*, 162–170.

(2) (a) Zhao, H.; Qu, Z. R.; Ye, H. Y.; Xiong, R. G. *Chem. Soc. Rev.* **2008**, *37*, 84–100. (b) Zhang, J.-P.; Chen, X.-M. *Chem. Commun.* **2006**, 1689–1699. (c) Lu, J. Y. *Coord. Chem. Rev.* **2003**, *246*, 327–347. (c) Zhang, X. M. *Coord. Chem. Rev.* **2005**, *249*, 1201–1219. (d) Xiong, R. G.; Xue, X.; Zhao, H.; You, X. Z.; Abrahams, B. F.; Xue, Z. L. *Angew. Chem., Int. Ed.* **2002**, *41*, 3800–3803.

(3) (a) Zheng, S. T.; Wang, M. H.; Yang, G. Y. *Inorg. Chem.* **2007**, *46*, 9503–9508. (b) Li, M.; Li, Z.; Li, D. *Chem. Commun.* **2008**, 3390–3392. (c) Han, Z. B.; He, Y. K.; Ge, C. H.; Ribas, J.; Xu, L. *Dalton Trans.* **2007**, 3020–3024. (d) Wang, J.; Zheng, S. L.; Hu, S.; Zhang, Y. H.; Tong, M. L. *Inorg. Chem.* **2007**, *46*, 795–800. (e) Weng, D. F.; Mu, W. H.; Zheng, X. J.; Fang, D. C.; Jin, L. P. *Inorg. Chem.* **2008**, *47*, 1249–1251.

(4) (a) Himo, F.; Demko, Z. P.; Noodleman, L.; Sharpless, K. B. *J. Am. Chem. Soc.* **2002**, *124*, 12210–12216. (b) Himo, F.; Demko, Z. P.; Noodleman, L.; Sharpless, K. B. *J. Am. Chem. Soc.* **2003**, *125*, 9983–9987.

(5) (a) Horikoshi, R.; Mochida, T.; Moriyama, H. *Inorg. Chem.* **2002**, *41*, 3017–3024. (b) Humphrey, S. M.; Mole, R. A.; Rawson, J. M.; Wood, P. T. *Dalton Trans.* **2004**, 1670–1678.

(6) (a) Horikoshi, R.; Mochida, T. *Coord. Chem. Rev.* **2006**, *250*, 2595–2609. (b) Tabellion, F. M.; Seidel, S. R.; Arif, A. M.; Stang, P. J. *J. Am. Chem. Soc.* **2001**, *123*, 7740–7741. (c) Horikoshi, R.; Mikuriya, M. *Cryst. Growth Des.* **2005**, *5*, 223–230. (d) Yan, L. *Z. Kristallogr.—New Cryst. Struct.* **2008**, *223*, 533–534. (e) Luo, J. H.; Hong, M. C.; Wang, R. H.; Yuan, D. Q.; Cao, R.; Han, L.; Xu, Y. Q.; Lin,

Z. Z. *Eur. J. Inorg. Chem.* **2005**, *44*, 1751–1758. (f) Yang, X. G.; Li, D. S.; Fu, F.; Tang, L.; Yang, J. Y.; Wang, L. L.; Wang, Y. Y. *Z. Anorg. Allg. Chem.* **2008**, *634*, 2634–2638.

(7) (a) Wang, J.; Zheng, S. L.; Hu, S.; Zhang, Y. H.; Tong, M. L. *Inorg. Chem.* **2007**, *46*, 795–800. (b) Han, L.; Bu, X. H.; Zhang, Q. C.; Feng, P. Y. *Inorg. Chem.* **2006**, *45*, 5736–5738. (c) Ma, L. F.; Wang, L. Y.; Du, M. *CrystEngComm* **2009**, *11*, 2593–2596. (d) Aragoni, M. C.; Arca, M.; Crespo, M.; Devillanova, F. A.; Hursthouse, M. B.; Huth, S. L.; Isaia, F.; Lippolis, V.; Verani, G. *CrystEngComm* **2007**, *9*, 873–878. (e) Ma, L. F.; Wang, Y. Y.; Wang, L. Y.; Lu, D. H.; Batten, S. R.; Wang, J. G. *Cryst. Growth Des.* **2009**, *9*, 2036–2038.

(8) Hao, Z. M.; Zhang, X. M. *Cryst. Growth Des.* **2007**, *7*, 64–68.

(9) (a) Kitagawa, H.; Ozawa, Y.; Toriumi, K. *Chem. Commun.* **2010**, *46*, 6302–6304. (b) Dias, H. V. R.; Diyabalanage, H. V. K.; Rawashdeh-Omary, M. A.; Franzman, M. A.; Omary, M. A. *J. Am. Chem. Soc.* **2003**, *125*, 12072–12073. (c) Ouellette, W.; Prosvirin, A. V.; Chieffo, V.; Dunbar, K. R.; Hudson, B.; Zubieta, J. *Inorg. Chem.* **2006**, *45*, 9346–9366. (d) Kobayashi, A.; Hara, H.; Noro, S.; Kato, M. *Dalton Trans.* **2010**, *39*, 3400–3406. (e) Hardt, H. D.; Pierre, A. *Z. Anorg. Allg. Chem.* **1973**, *402*, 107–112. (f) Ford, P. C.; Cariati, E.; Bourassa, J. *Chem. Rev.* **1999**, *99*, 3625–3648. (g) Harvey, P. D.; Knorr, M. *Macromol. Rapid Commun.* **2010**, *31*, 808–826. (h) Knorr, M.; Pam, A.; Khatyr, A.; Strohmann, C.; Kubicki, M. M.; Rousselin, Y.; Aly, S. M.; Fortin, D.; Harvey, P. D. *Inorg. Chem.* **2010**, *49*, 5834–5844.

(10) (a) Zhu, Q. L.; Sheng, T. L.; Fu, R. B.; Hu, S. M.; Chen, L.; Shen, C. J.; Ma, X.; Wu, X. T. *Chem.—Eur. J.* **2011**, *17*, 3358–3362. (b) Zhu, Q. L.; Sheng, T. L.; Fu, R. B.; Hu, S. M.; Chen, J. S.; Xiang, S. C.; Shen, C. J.; Wu, X. T. *Cryst. Growth Des.* **2009**, *9*, 5128–5134.

(11) Hoog, P. De.; Gamez, P.; Driessen, W. L.; Reedijk, J. *Tetrahedron Lett.* **2002**, *43*, 6783–6786.

(12) Sheldrick, G. M. *SHELXTL NT Version 5.1. Program for the Solution and Refinement of Crystal Structures*; University of Göttingen: Göttingen, Germany, 1997.

(13) (a) Wang, J.; Zhang, Y. H.; Li, H. X.; Lin, Z. J.; Tong, M. L. *Cryst. Growth Des.* **2007**, *7*, 2352–2360. (b) Morine, G. H.; Kuntz, R. R. *Photochem. Photobiol.* **1981**, *33*, 1–5.

(14) Vaganova, E.; Wachtel, E.; Rozenberg, H.; Khodorkovsky, V.; Leitus, G.; Shimon, L.; Reich, S.; Yitzchaik, S. *Chem. Mater.* **2004**, *16*, 3976–3979.

(15) Zhu, Q. L.; Sheng, T. L.; Fu, R. B.; Hu, S. M.; Shen, C. J.; Ma, X.; Wu, X. T. *CrystEngComm* **2011**, *13*, 2096–2105.

(16) (a) Braga, D.; Maini, L.; Mazzeo, P. P.; Ventura, B. *Chem.—Eur. J.* **2010**, *16*, 1553–1559. (b) Fang, Q. R.; Zhu, G. S.; Jin, Z.; Ji, Y. Y.; Ye, J. W.; Xue, M.; Yang, H.; Wang, Y.; Qiu, S. L. *Angew. Chem., Int. Ed.* **2007**, *46*, 6638–6642. (c) Tam, A. Y. Y.; Wong, K. M. C.; Yam, V. W. W. *J. Am. Chem. Soc.* **2009**, *131*, 6253–6260.

(17) (a) Hao, Z. M.; Fang, R. Q.; Wu, H. S.; Zhang, X. M. *Inorg. Chem.* **2008**, *47*, 8197–8203. (b) Sun, D.; Wang, D. F.; Han, X. G.; Zhang, N.; Huang, R. B.; Zheng, L. S. *Chem. Commun.* **2011**, *47*, 746–748. (c) Zhang, J. P.; Qi, X. L.; Liu, Z. J.; Zhu, A. X.; Chen, Y.; Wang, J.; Chen, X. M. *Cryst. Growth Des.* **2011**, *11*, 796–802.

(18) Paw, W.; Lachicotte, R. J.; Eisenberg, R. *Inorg. Chem.* **1998**, *37*, 4139–4141.

(19) (a) Muthu, S.; Ni, Z.; Vittal, J. J. *Inorg. Chim. Acta* **2005**, *358*, 595–605. (b) Hao, Z. M.; Zhang, X. M. *Cryst. Growth Des.* **2007**, *7*, 64–68.

(20) Jung, O.; Park, S. H.; Park, C. H.; Park, J. K. *Chem. Lett.* **1999**, *8*, 923–924.

(21) (a) Fang, Q. R.; Zhu, G. S.; Jin, Z.; Ji, Y. Y.; Ye, J. W.; Xue, M.; Yang, H.; Wang, Y.; Qiu, S. L. *Angew. Chem., Int. Ed.* **2007**, *46*, 6638–6642. (b) Sun, Y.; Ye, K.; Zhang, H.; Zhang, J.; Zhao, L.; Li, B.; Yang, G.; Yang, B.; Wang, Y.; Lai, S. W.; Che, C. M. *Angew. Chem., Int. Ed.* **2006**, *45*, 5610–5613.

(22) (a) Sun, D. F.; Ke, Y. X.; Collins, D. J.; Lorigan, G. A.; Zhou, H. C. *Inorg. Chem.* **2007**, *46*, 2725–2734. (b) Gao, W.; Xing, F. F.; Zhou, D.; Shao, M.; Zhu, S. R. *Inorg. Chem. Commun.* **2011**, *14*, 601–605. (c) Sun, D. F.; Ma, S. Q.; Ke, Y. X.; Petersen, T. M.; Zhou, H. C. *Chem. Commun.* **2005**, 2663–2665.

(23) Lee, J. Y.; Lee, S. Y.; Sim, W.; Park, K.; Kim, J.; Lee, S. S. *J. Am. Chem. Soc.* **2008**, *130*, 6902–6903.